

Invited Paper

Challenges of 3-D characterization of polymer-based drug delivery devices with cluster Secondary Ion Mass Spectrometry

Christine M. Mahoney,^{1*} Albert J. Fahey¹, Anna M. Belu², and Joseph A. Gardella Jr.³

¹ National Institute of Standards and Technology, 100 Bureau Drive, Mail Stop 8371, Gaithersburg, Maryland 20899

² Medtronic Inc., 710 Medtronic Parkway, LT130, Minneapolis, Minnesota 55432-5604

³ Department of Chemistry, State University of New York at Buffalo, Buffalo, New York 14260-3000

*christine.mahoney@nist.gov

(Received : October 3, 2010; Accepted : December 30, 2010)

Three-dimensional (3-D) molecular imaging in polymeric biomaterials, particularly in the near surface region (1 nm to 500 nm), is extremely important for drug delivery applications, as these regions play a vital role in both the biocompatibility and drug release characteristics in drug delivery systems. Although pharmaceutical companies typically use dissolution studies to monitor the rate of drug release, these studies need to be correlated with actual structural information, compositions and defects within the device. This work discusses the most recent advances and challenges in utilizing Cluster Secondary Ion Mass Spectrometry (cluster SIMS) for 3-D characterization and quantification in polymer-based drug delivery systems. The results are promising, showing the ability to quantify and image the 3-dimensional distribution of drugs in polymer layers. However, many problems still remain in terms of analysis of real-world samples, including complex sample geometries, ionization effects, and beam-induced sample damage. These problems, and how to address them, are discussed briefly here.

1. Introduction

Over the past decade, Secondary Ion Mass Spectrometry (SIMS) has proven to be a powerful analytical tool for surface and in-depth molecular characterization of polymer materials [1]. This is in large part a result of the advent of polyatomic primary ion sources, such as C_{60}^{n+} , SF_5^+ , and $Ar_{(n>100)}^+$. [2,3,4] Because of their surface localized damage regime, polyatomic primary ion sources, or “cluster” sources have enabled the analyst to sputter depth profile in soft materials; an ability previously unattainable using the more conventional atomic beams [1,2,3,4,5,6].

A very promising application of cluster SIMS is the surface and in-depth characterization of polymeric biomaterials [6,7,8,9,10,11,12,13]. An example is given in Figure 1 which illustrates the capability of cluster SIMS for depth profiling in a model drug eluting stent system comprised of rapamycin in a poly(lactic acid) (PLA) matrix [8,13]. In the figure, the diffusion profiles of the rapamycin at the surface and interface regions are clearly observed [3], where the signal characteristic of the rapamycin (green) is most intense at the surface. The drug signal then decays

to a minimum, a point referred to as the drug depletion zone, and then increases again to the bulk concentration region. It is expected that the concentration in the bulk region will be consistent with the actual mass fraction of drug in the film (50% in this case). Finally, an interfacial diffusion profile is also observed, showing segregation of the drug to the PLA/Si interface. The polymer signal (red) also varies with sputter time, and behaves commensurately with the rapamycin signal. A 2-D slice overlay of these secondary ion signals as a function of depth (z) is displayed in Fig. 1b. Here the distribution of the drug in the film is clearly observed.

Although these results appear to be very promising for drug delivery applications, the application of cluster SIMS for depth profiling in real-world samples is not without its difficulties. This paper will address some specific challenges often faced in the areas of; 1) complex real world geometries, 2) quantitative depth profiling, 3) the gel point limitation, and 4) matrix effects in protein-based drug delivery devices.

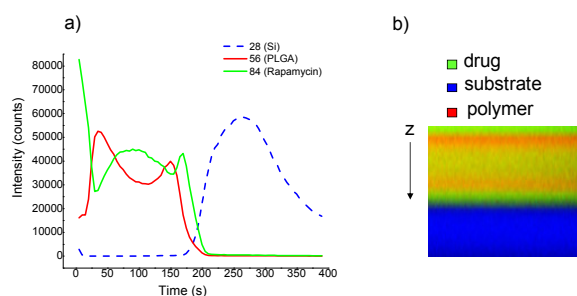


Fig. 1. Representative depth profile of a thin film (200 nm), containing rapamycin (drug) in a poly(lactic acid) (PLA) matrix (mass fraction = 50%). a) Average intensity profiles of m/z 56 (PLGA), m/z 84 (rapamycin) and m/z 28 (Si substrate), and (b) z -scale image showing the distribution of the drug in the PLA.

2. Experimental

Secondary Ion Mass Spectrometry. All SIMS experiments were performed on an Ion-TOF IV* (Munster, Germany) Time-of-Flight Secondary Ion Mass Spectrometer equipped with both Bi_3^+ and SF_5^+ primary ion beam sources. The analysis source was a pulsed 25 keV Bi_3^+ beam, which bombarded the surface at an incident angle of 45° to the surface normal. The target current was maintained at ≈ 2 pA throughout all experimentation. The sputter source was a continuous SF_5^+ primary ion beam operated under similar geometries, but at higher currents (nA) in order to enable efficient sputter removal. The beam energies, raster sizes, and beam currents varied depending on the experiment and are specified below. All experiments utilized a low energy electron beam for charge compensation.

Model drug eluting stent films. PLA/Rapamycin films were prepared by spin coating (209.7 rad/s for 30 s) solutions of PLA and rapamycin in chloroform, where the mass fraction of PLA in the solution was 1%, and the mass fraction of rapamycin relative to PLA was 50%. 5 keV SF_5^+ was utilized at 5 s intervals with a raster size of $750 \mu\text{m} \times 750 \mu\text{m}$. The current of the SF_5^+ source was maintained at ≈ 3 nA throughout the depth profile. Each sputter interval was immediately followed by a 5 s Bi_3^+ analysis interval using a $200 \mu\text{m} \times 200 \mu\text{m}$ rastered area.

* Certain commercial equipment, instruments or materials are identified in this article to specify adequately the experimental procedure. Such identification does not imply recommendation or endorsement by the National Institute of Standards and Technology, nor does it imply that the materials or equipment identified are necessarily the best available for the purpose.

PLA/Rapamycin depth profile experiments were performed at -100°C to avoid the accumulation of damage.

Pluronic/PLA blends. Pluronic/PLA blends were prepared by spin coating (104.7 rad/s for 30 s) solutions in chloroform. Solid fractions were maintained at 5%, where the mass fraction of pluronic (P104) in the films was varied (0%, 1%, 3%, 5%, 10%, 15%, 25%, 50%). These conditions resulted in average films thicknesses of $\approx 1.2 \mu\text{m}$. Depth profiles were performed using 8 keV SF_5^+ at 5 s sputter intervals, ≈ 6 nA continuous current, and a $750 \mu\text{m} \times 750 \mu\text{m}$ raster size. Each sputter interval was followed immediately by a 5 s pause to allow for charge dissipation prior to analysis with the Bi_3^+ beam. The Bi_3^+ analysis interval comprised of 3 complete scans at 128×128 pixel resolution. Depth scale conversions were performed by dividing the depth of the film (as determined by stylus profilometry) [6] by the total sputtering time required to reach the derivative of the Si curve. P104/PLA blend systems were depth profiled at -100°C to avoid the accumulation of damage.

Gel point studies. Gel point studies were performed using 8 keV SF_5^+ operated at 8 nA continuous current and a $300 \mu\text{m} \times 300 \mu\text{m}$ raster. Craters were sputtered for 10 minutes under the conditions specified, and then removed from the instrument. The wafers containing the craters were then exposed to a 1:1 acetone/methanol mixture for 3 min. The wafer was then removed and subsequently analyzed using SIMS analysis and optical microscopy.

Insulin containing blends. To make three component blends of P104, PLA and insulin, two solutions were prepared. The first solution, containing P104 and PLA at a total solids content of 2 %, was prepared in methylene chloride. The P104 mass fraction (X_{P104}) in this solution was maintained at 15 %. This solution served as the “oil phase”. A second “water phase” solution was also prepared (insulin content of 2 %. Immediately after the oil phase was added to the water phase (18:1, respectively), the two phases were emulsified. Each resulting emulsion was spin cast onto a silicon substrate at 157 rad/s for 30 s immediately after the mixing. The cast films were then introduced into the SIMS vacuum chamber for analysis. For more information about the resulting SIMS experiments, see references [10].

3. Results and Discussion

Real-world geometries. The depth profile displayed in Fig. 1 was taken from an optimal

system for SIMS analysis, in that the films were smooth films spun cast onto Si substrates. Unfortunately, real-world drug delivery systems typically have more complex geometries, are thicker films (in the cases where the drug delivery system is a coating), or are bulk insulating systems (such as drug capsules). These systems may be much more difficult if not impossible to measure in 3-dimensions. Furthermore, drug delivery devices will often contain many additives, binders, and other excipients, masking the relevant signals and making them much more difficult to depth profile. These complex mixtures will likely have components that have different sputter properties, such that preferential sputtering occurs in certain areas of the device as compared to other areas. There also will likely be a variety of surface contaminants, although many of these contaminants can be easily removed via sputtering [1].

An example of the geometry issue is discussed in reference [8], where the attempt is made to depth profile through a cylindrical shaped drug-eluting stent. The stent coating in this reference was comprised of the same materials discussed in Fig. 1. However, due to the geometry of the stent, the depth profile results were less than optimal. This is because the local electric field in non-flat surfaces is non-uniform, thus changing the secondary ion trajectories. It may be useful in such examples; to analyze the raw data for specified regions of interest that have similar ion trajectories, as was done in reference 8. Furthermore, the ion beam geometries in these types of experiments should be such that the sputter gun is on the same side as the analysis gun.

Although depth profiling proved to be rather difficult for this system, surface analysis was still useful, detecting large amounts of drug at the surface in the 25% and 50% formulations, much less in the 5% formulation, and none at all in the capped coating (25% formulation, capped with pure PLGA overlayer).

Quantification of organic depth profiles.

Much has been published in the area of polymer depth profiling with cluster ion beams over the past decade [1]. However, there has not been much in the way of quantitative depth profiling in these systems. One example of quantitative analysis in polymer systems has been reported on for a series of pluronic/PLA blend systems potentially utilized for protein drug delivery applications [3]. In these systems, the pluronic component (P104), a triblock copolymer consisting of poly(ethylene oxide) (PEO) and

poly(propylene oxide) (PPO) components, tends to preferentially segregate to the surface. These experiments have been repeated here using a Bi_3^+ cluster ion source (as opposed to Ar^+ which was utilized in the previous work) under different experimental conditions (i.e. low temperatures during analysis, and thicker films), and with a different set of peaks selected for more accurate quantification in the surface region. Fig. 2 shows the depth profile results for a PLA/P104 blend system containing a P104 mass fraction of 10%. Fig. 2a plots the intensities characteristic of P104 (m/z 59), PLA (m/z 56), and Si (m/z 28) as a function of SF_5^+ sputter time. The depth profile clearly shows preferential segregation of the P104 components to the surface and interface regions, similar to earlier results [3].

The corresponding quantitative data is displayed in Fig. 2b, which shows the P104 mass fraction (%) plotted as a function of depth for the system depth profiled in (a), where the composition of the surface has been verified by X-Ray Photoelectron Spectroscopy (XPS). This concentration depth profile was obtained by preparing calibration curves from a series of samples containing varying amounts of P104. The intensity ratios of P104 (m/z 59) to PLA (m/z 56) were plotted as a function of depth for each

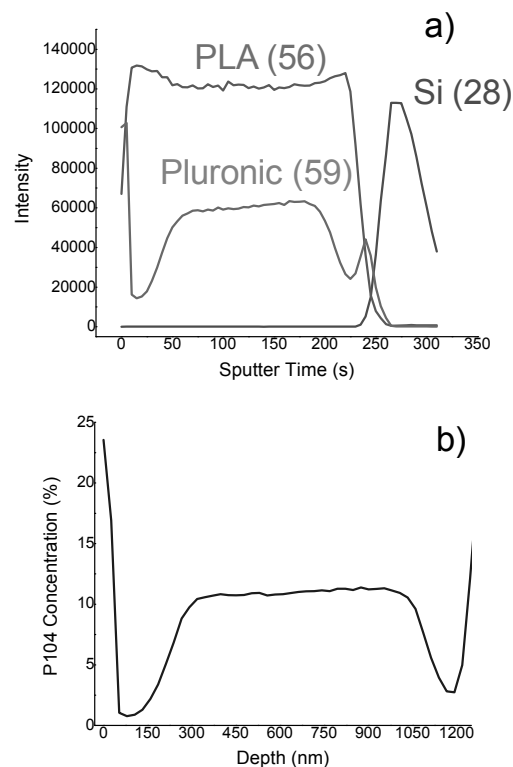


Fig. 2. Intensity profiles (a), and P104 concentration depth profiles (b) for a 1 μm thick film (on Si) of PLA containing P104 at a mass fraction of 10%.

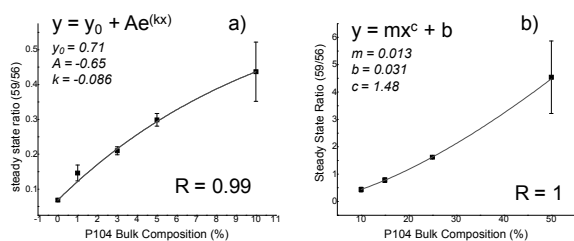


Fig. 3. Steady state ratios of m/z 59 (P104) to m/z 56 (PLA) plotted as a function of known P104 bulk composition for P104 mass fractions of (a) 0%, 1%, 3%, 5% and 10%, and (b) 10%, 15%, 25% and 50%. Each point represents an average taken from 4 separate measurements, where the error bars represent the standard deviations. (a) was fitted to an exponential function, while (b) was fitted to a power function. These fitting parameters and equations were used to obtain the concentration depth profile shown in Fig. 2b.

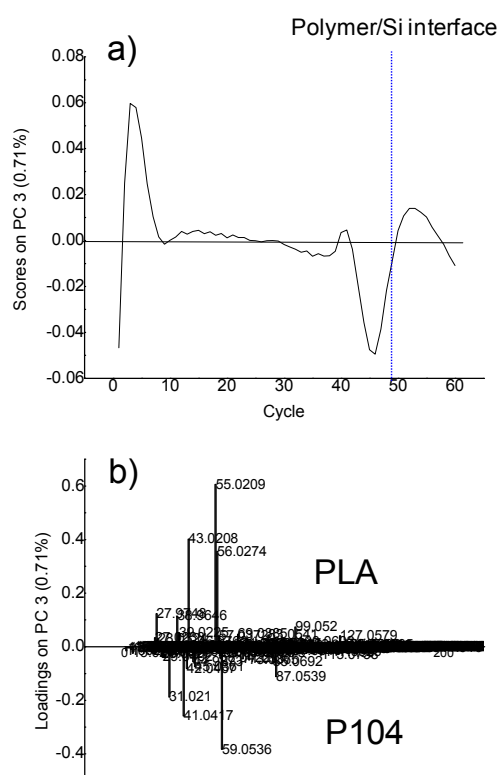


Fig. 4. (a) scores, and (b) loadings plots for principal component 3 (PC3), obtained from the complete mass spectral dataset obtained during a depth profiling experiment of a P104 / PLA blend matrix containing a P104 mass fraction of 25%.

sample. The average intensity ratio in the steady-state region of the profile was then plotted as a function of known bulk concentration under the assumption that the concentration in the steady state region was approximately equal to the known bulk content. The resulting calibration curves are plotted in Fig. 3. As can be seen, and as is typical in SIMS experiments involving

quantification, these curves are not linear, and behave quite differently under different concentration ranges. However, the curves showed a very good fit to the selected models, as indicated by the R-values reported in the graphs.

Another way to obtain useful data from depth profiling of drug delivery systems is to use principal components analysis (PCA) [14]. Fig. 4 shows an example of how one can use PCA for analyzing depth profiling data from the PLA/P104 blend systems. Fig. 4a depicts scores (principal component 3) from the PCA analysis of a PLA/P104 blend depth profile containing a bulk P104 mass fraction of 25%. The scores are plotted as a function of depth profile cycle, where the polymer/Si interface is indicated by the vertical dashed line. These scores are correlated with the corresponding loadings plot in Fig. 4b, where the positive scores are correlated with positively loaded peaks; peaks characteristic of the PLA component, and the negative scores are correlated with negatively loaded peaks; peaks characteristic of the P104 component.

PCA is a very nice way to characterize the complete mass spectral dataset in a given depth profile, for it provides insight into changes occurring in the dataset that may be overlooked otherwise. Principal component 3 (PC3), which is shown in Fig. 4 describes the variance between PLA and P104 peaks. However, there were up to 6 components observed in the data which showed other changes attributed to Si (PC1), K (PC2), hydrocarbon contaminants (PC5) and even the oxide layer on the Si (PC6). For more information on PCA, please see references [14].

Delaying the Gel Point. The effects of ion beam irradiation on polymer chemistry plays a very important role in depth profile results [1]. Fig. 5a illustrates a model depth profile in a bulk polymer, with corresponding structural changes shown in Fig. 5b. In the early stages of ion bombardment (region I), there is a surface transient region, which describes the initial decay associated with the damage saturation process [15,16]. After this initial change, there is a stabilization of the signal intensity (region II), which represents the region where the damage created by the ion beam is at equilibrium with the sputter removal of that damage [15]. The predominant “damage” mechanism in region II is a random main-chain scission process (see corresponding structure in Fig. 5b), yielding low molecular weight products with increased solubility[1]. Though main chain scission is the dominant mechanism in this region, it is important

to understand that some cross-links are also formed (see Fig. 5b), and the number of these cross-links will accumulate with dose. As the number of cross-links in a polymer increases, the secondary ion yields and sputter yields will also decrease [1,17,18]. In cases where cross-linking plays a more dominant role, the signal in this region will steadily decline with increasing dose. Eventually, after a critical number of cross-links are formed, such that a 3-D network is formed (gel-point)[1], the cross-linking mechanisms rapidly accelerate, resulting in a sudden loss of secondary ion signal intensities (region III). Finally, at higher doses, a graphitization process begins (region IV),

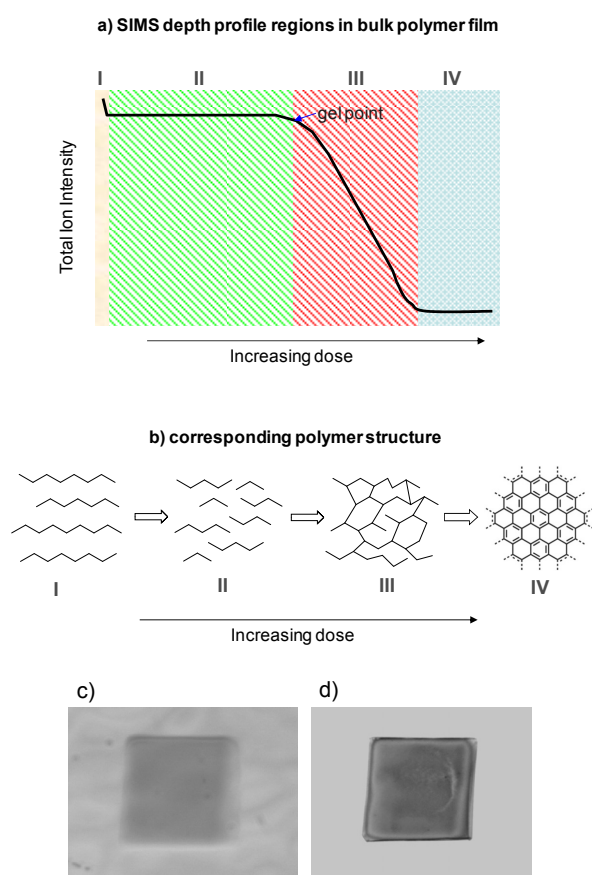


Fig. 5. Damage processes in polymers during ion bombardment: (a) representative SIMS depth profile of polymer, with four regions; I) surface transient region, II) steady-state region, III) gel point region, and IV) graphitization region. (b) corresponding polymeric structure with (a). (c) optical image of 300 μm x 300 μm high dose SF_5^+ PMMA crater bottom (sputtered beyond the gel point of the polymer). (d) optical image of crater in (c) after soaking in 1:1 methanol:acetone for 3 minutes. Bright areas in the image are the Si substrate. All the polymer surrounding the crater has been removed.

accompanied by an increased conductivity of the surface and the presence of graphitic type peaks in the mass spectrum.

Fig. 5c and Fig. 5d show images of SF_5^+ sputtered crater bottoms under high primary ion dose conditions (see experimental for details) before and after exposing the films to a 1:1 acetone : methanol solution for 3 minutes. It is well known that gels will swell in solvents, but will not dissolve. As can be seen, the crater remains intact after exposure to the solvent, while all of the surrounding undamaged PMMA has been removed. The corresponding SIMS images of the crater bottoms after soaking show signal characteristic of PMMA (m/z 59) localized to the crater, and Si signal (m/z 28) in the background. This confirms that sputtering at higher primary ion doses, does indeed cause the formation of an insoluble polymer gel. Therefore, it is very important in depth profiling of polymeric biomaterials, to delay the gel point. There are several important variables that will help to do this, including using a different ion source, increasing the ion beam energy, decreasing the temperature during the depth profile process, changing the ion beam incidence angle, and changing the ambient environment [1]. All of these factors need to be considered before performing any depth profile in a polymer system. It should be noted that the $\text{Ar}_{(n>100)}^+$ ion source is proving to be very efficient for polymer sputter removal prior to the gel point, and in fact, no such effect has yet been observed when using this source [19].

Decreased Sensitivity for Proteins in drug delivery systems. One of the most difficult barriers to overcome during depth profiling of polymeric drug delivery devices remains to be the effect of relative ionization efficiencies in multicomponent systems. A very important example in drug delivery is observed in the very competitive field of protein drug delivery. Delivery of proteins, and other water soluble macromolecular drugs, is a very difficult process. This is in large part due to the decreased stability and bioavailability of the proteins in certain drug delivery vehicles. 3-D molecular analysis could play a critical role in this field. However, the primary issue is that the proteins do not ionize well with SIMS.

A good example of this is shown in Fig. 6. This system is the same pluronic/PLA blend system described earlier. However, in this case, the system also contains 5% insulin. The secondary ion images of P104 (m/z 59) and PLA (m/z 56) are plotted as a function of increasing

sputter time (depth) in Fig. 6b. The 3-dimensional distribution is readily observed, and is consistent with the formation of pluronic micelles which protect the insulin protein from the hydrophobic PLA matrix. However, no protein signals, or amino acid signals were detected in this experiment [10]. More recent attempts to image Bovine Serum Albumin in this system have also been unsuccessful. Corresponding negative ion images do in some cases show increased amount of CN⁻ signal in these regions. However, molecular imaging in these regions remains elusive. Attempts are currently underway to enhance the ionization of proteins relative to the PLA matrix in these systems.

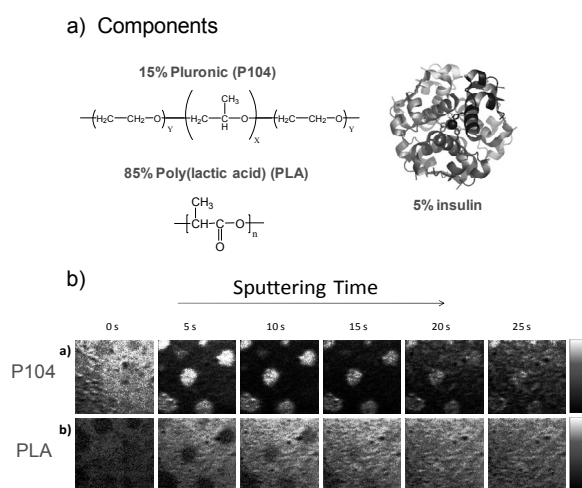


Fig. 6. Image depth profiling (300 μm x 300 μm) in 3-component blend. (a) structures and compositions of polymer blend / insulin system, and (b) positive secondary ion image maps of m/z 59 (top – P104), and m/z 56 (bottom – PLA).

4. Conclusions

3-D analysis of polymeric-based drug delivery systems with cluster primary ion sources is proving to be very successful. However, there are still areas which need significant work in terms of SIMS analysis of real-world systems. These problems however are not insurmountable, and it is expected that many advancements will be made over the coming years, that will allow for rapid and robust 3-D molecular characterization in any drug delivery system, regardless of geometry, dosage form, or complexity of the system.

5. References

- [1] C.M.Mahoney. *Mass Spectrom Rev* **29(2)**, 247-293 (2010).
- [2] C.Szakai, S. Sun, A. Wucher, and N. Winograd. *Applied Surface Science* **231-232**, 183-185 (2004).
- [3] C.M.Mahoney, J. Yu, and J. A. Gardella, Jr. *Anal Chem* **77(11)**, 3570-3578 (2005).
- [4] S.Ninomiya, K. Ichiki, H. Yamada, Y. Nakata, T. Seki, T. Aoki, and J. Matsuo. *Rapid communications in mass spectrometry: RCM* **23(20)**, 3264 (2009).
- [5] A.Delcorte, B. J. Garrison, and K. Hamraoui. *Anal Chem* **81(16)**, 6676-6686 (2009).
- [6] C.M.Mahoney, S. V. Roberson, and G. Gillen. *Anal Chem* **76(11)**, 3199-3207 (2004).
- [7] G.L.Fisher, A. M. Belu, C. M. Mahoney, K. Wormuth, and N. Sanada. *Anal Chem* **81(24)**, 9930-9940 (2009).
- [8] C.M.Mahoney, A. J. Fahey, and A. M. Belu. *Anal Chem* **80(3)**, 624-632 (2008).
- [9] C.M.Mahoney, D. V. Patwardhan, and M. K. McDermott. *Applied Surface Science* **252(19)**, 6554-6557 (2006).
- [10] C.M.Mahoney, J. X. Yu, A. Fahey, and J. A. Gardella. *Applied Surface Science* **252(19)**, 6609-6614 (2006).
- [11] S.A.Burns, R. Hard, W. L. Hicks Jr, F. V. Bright, D. Cohan, L. Sigurdson, and J. A. Gardella Jr. *Journal of Biomedical Materials Research Part A* **94(1)**, 27-37 (2010).
- [12] R.M.Braun, J. Cheng, E. E. Parsonage, J. Moeller, and N. Winograd. *Anal Chem* **78(24)**, 8347-8353 (2006).
- [13] A.Belu, C. Mahoney, and K. Wormuth. *J Control Release* **126(2)**, 111-121 (2008).
- [14] M.S.Wagner, D. J. Graham, B. D. Ratner, and D. G. Castner. *Surface Science* **570(1-2)**, 78-97 (2004).
- [15] A.Wucher and N. Winograd. *Anal Bioanal Chem* **396(1)**, 105-114 (2010).
- [16] G.Gillen, D. S. Simons, and P. Williams. *Anal Chem* **62(19)**, 2122-2130 (1990).
- [17] M.S.Wagner, K. Lenghaus, G. Gillen, and M. J. Tarlov. *Applied Surface Science* **253(5)**, 2603-2610 (2006).
- [18] A.Chilkoti, G. P. Lopez, B. D. Ratner, M. J. Hearn, and D. Briggs. *Macromolecules* **26(18)**, 4825-4832 (1993).
- [19] S.Ninomiya, K. Ichiki, H. Yamada, Y. Nakata, T. Seki, T. Aoki, and J. Matsuo. *Rapid communications in mass spectrometry: RCM* **23(11)**, 1601 (2009).